Hindawi
International Journal of Corrosion
Volume 2018, Article ID 9212705, 15 pages
https://doi.org/10.1155/2018/9212705

*Research Article*

# Electrochemical Studies of Monoterpenic Thiosemicarbazones as Corrosion Inhibitor for Steel in 1 M HCl

**R. Idouhli**,[1] **A. N'Ait Ousidi**,[2] **Y. Koumya**,[1] **A. Abouelfida**,[1] **A. Benyaich**,[1] **A. Auhmani**,[2] **and Moulay Youssef Ait Itto**[2]

[1]*Laboratory of Physical Chemistry of Materials and Environment, Department of Chemistry, Faculty of Science Semlalia, Cadi Ayyad University, BP 2390, Marrakech, Morocco*
[2]*Organic Synthesis and Molecular Physico-Chemistry Laboratory, Department of Chemistry, Faculty of Science Semlalia, Cadi Ayyad University, BP 2390, 40001 Marrakech, Morocco*

Correspondence should be addressed to A. Benyaich; benyaich@uca.ac.ma

Received 8 November 2017; Accepted 8 February 2018; Published 1 January 1

Academic Editor: Tuan Anh Nguyen



We have studied the inhibitory effect of some Monoterpenic Thiosemicarbazones on steel corrosion in 1 M HCl solution. The potentiodynamic polarization and electrochemical impedance spectroscopy were used. The Monoterpenic Thiosemicarbazones have inhibited significantly the dissolution of steel. The inhibition efficiency increased with increasing inhibitor concentration and also with the increase in temperature (293–323 K). Furthermore, the results obtained revealed that the adsorption of inhibitor on steel surface obeys Langmuir adsorption model and the thermodynamic parameters such as enthalpy and activation energy were determined. The scanning electron microscopy combined with dispersive X-ray spectroscopy examinations were used to see the shape of the surface morphology and to determine the elemental composition. Scanning electron microscope (SEM) images show that the surface damage decreases when the inhibitor is added. The quantum chemical calculations using density functional theory (DFT) were performed in order to provide some insights into the electronic density distribution as well as the nature of inhibitor-steel interaction.

## 1. Introduction

Corrosion problems have sparked a considerable attention because of their aggressiveness towards materials [1]. The most important application of steel is in the oil and gas pipelines, refineries, recovery units, and so forth. Acid solutions are usually used as acid pickling, acid descaling, and industrial acid cleaning [2]. The use of inhibitors is one of the best ways to protect metals and alloys against corrosion in acidic medium [3, 4]. The environmental toxicity of organic products has prompted the search for new eco-friendly substances readily available and effective molecules having very high inhibition efficiency [5, 6]. It is well known that organic compounds containing heteroatoms, such as sulfur, nitrogen, and oxygen, could be excellent for corrosion inhibitors [7]. The efficiency of these organic inhibitors is related to their ability to be adsorbed on metal surface which is influenced by some of their electronic and physicochemical properties such as electronic structure, steric factor, aromaticity, electronic density at donor site, and presence of functional groups [8, 9]. The inhibition process could be explained by a physical or chemical adsorption of these organic molecules into the surface of the metal, forming a protective layer to isolate the metal from the corrosion [10]. Some researchers explain that the inhibition process is related to the formation of donor-acceptor surface complexes between a vacant d-orbital of metal and $\pi$ or free electron inhibitor containing heteroatoms [11, 12]. Moreover, in recent years, the thiosemicarbazones as corrosion inhibitors have been widely studied and have shown their good inhibition efficiency [13–17]. In addition, these compounds have demonstrated high potency inhibition that related to the presence of sulfur and nitrogen. These explain their ability to form complexes with different metals especially with steel [16, 18]. In addition to experimental studies, the density functional theory (DFT) is widely used to

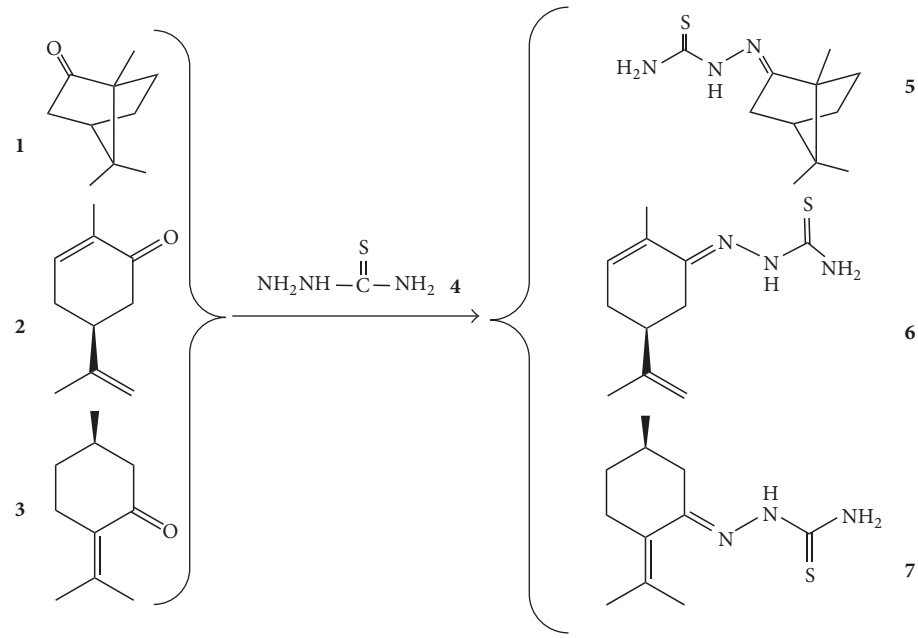


Figure 1: Chemical structure of the Monoterpenic Thiosemicarbazones **(5–7)** and their synthesis from the corresponding naturally occurring monoterpenes **(1–3)**.

interpret the experimental results of the observed inhibition [8].

The aim of this work is to evaluate the corrosion kinetic parameters of steel and the adsorption thermodynamic parameters of some Monoterpenic Thiosemicarbazones in 1 M HCl solution. The polarization curves and the electrochemical impedance spectroscopy were used. The morphology of steel was checked before and after experiments by scanning electron microscopy (SEM) and the surface composition was analyzed using energy dispersive X-ray (EDX) spectroscopy. The corrosion inhibition effect of the Monoterpenic Thiosemicarbazones was also investigated by theoretical calculations (DFT) and correlated with the experimental inhibition efficiencies.

## 2. Experimental

*2.1. Synthesis of Corrosion Inhibitors.* The Monoterpenic Thiosemicarbazones **(5–7)** were prepared according to the reported reaction in Figure 1 [19–21]. Chemical structure, molecular formula, molecular weight, analytical data, and chemical abbreviation used are given in Table 1.

*2.2. Preparation of Electrode and Solution.* The steel specimens were cut from a cylindrical rod with an exposed area of 0.76 $cm^2$ to electrolyte. The chemical composition of working electrode was Fe (98.55%), C (0.15%), Mn (1.25%), and Si (0.05%). Before each electrochemical experiment, the surface of steel specimens was mechanically abraded using different grades of abrasive paper (180, 500, and 1200 grades), degreased with acetone, and rinsed with distilled water. The electrolyte solution 1 M HCl was prepared from an analytical grade (37%) hydrochloric acid.

*2.3. Electrochemical Measurements.* Electrochemical measurements were carried out using a potentiostat PGZ100 piloted by voltamaster4 software. This potentiostat is connected to a double-walled one-compartment cell with a three-electrode configuration. A platinum electrode with 2 $cm^2$ surface area and Ag/AgCl were used as auxiliary and reference electrodes, respectively. The working electrode surface area exposed to the electrolyte was 0.76 $cm^2$. The open circuit potential was measured after 30 minutes until it reaches steady state conditions. The electrochemical impedance spectroscopy experiments were performed at corrosion potential in frequencies ranging from 100 KHz to 10 mHz by applying a sine wave voltage of 10 mV peak to peak with data density of 10 points per decade. The impedance parameters were calculated by fitting the experimental results to an equivalent circuit using EC-Lab software. The polarization curves were scanned in the range of −800 mV to −200 mV at a scanning rate of 1 $mV{\cdot}s^{-1}$. The effect of temperature on the inhibitor efficiency was controlled thermostatically in a temperature range of 293 at 323 K. Experiments were repeated many times to check the reproducibility and the average values presented.

*2.4. Surface Investigation.* The steel surface morphology was modified by immersion for 2 h, of the cleaned samples in 1 M HCl solution in absence and presence of inhibitor. After washing, the specimens were dried. The prepared coupons were used for surface analysis using scanning electron microscopy (SEM). The presence of surface elements was determined using high energy dispersive X-ray (EDX). The SEM with EDX analyses was carried out using VEGA3 LM TESCAN instrument at an accelerating voltage of 20 kV and 2.00kx magnification.

Table 1: IUPAC name, molecular structure, molecular formula, melting point, and analytical data of studied Monoterpenic Thiosemicarbazones.

| Name of inhibitor | Chemical structure | Analytical data |
|---|---|---|
| Camphor thiosemicarbazone **(5)** | 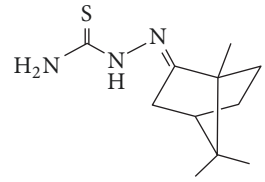 | *Chemical formula*: $C_{11}H_{19}N_3S$ *Exact mass*: 225.13 *Molecular weight*: 225.35 Solid m.p: 154-155°C |
| Carvone thiosemicarbazone **(6)** | 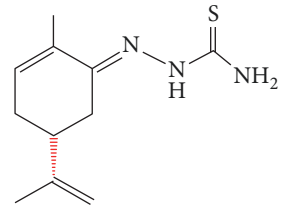 | *Chemical formula*: $C_{11}H_{17}N_3S$ *Exact mass: 223.11* *Molecular weight*: 223.34 Solid m.p: 111-112°C; |
| Pulegone thiosemicarbazone **(7)** | 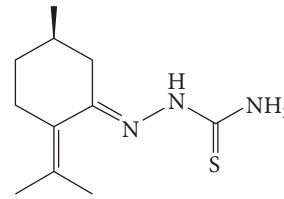 | *Chemical formula*: $C_{11}H_{19}N_3S$ *Exact mass*: 225.13 *Molecular weight*: 225.35 oil |

Table 2: Electrochemical parameters for the corrosion of steel in 1 M HCl containing different concentrations of Camphor thiosemicarbazone (5), Carvone thiosemicarbazone (6), and Pulegone thiosemicarbazone (7).

| Inhibitors | $C$ (mmol/L) | $i_{corr}$ (mA/cm$^2$) | $E_{corr}$ (mV) | $\beta a$ (mV/dec) | $\beta c$ (mV/dec) | $\eta$ (%) |
|---|---|---|---|---|---|---|
| | Blank | 0.6828 | −379 | 77 | −142 | — |
| (5) | 0.1 | 0.077 | −411 | 65 | −118 | 88.72 |
| | 0.5 | 0.071 | −392 | 89 | −189 | 89.60 |
| | 1.0 | 0.0694 | −391 | 78 | −120 | 89.84 |
| | 5.0 | 0.0334 | −438 | 116 | −170 | 95.11 |
| (6) | 0.1 | 0.0837 | −385 | 65 | −120 | 87.74 |
| | 0.5 | 0.0726 | −402 | 74 | −119 | 89.37 |
| | 1.0 | 0.0728 | −439 | 127 | −176 | 89.34 |
| | 5.0 | 0.0655 | −428 | 126 | −204 | 90.41 |
| (7) | 0.1 | 0.1979 | −430 | 59 | −107 | 71.00 |
| | 0.5 | 0.1554 | −389 | 42 | −172 | 77.24 |
| | 1.0 | 0.1325 | −381 | 31 | −154 | 80.59 |
| | 5.0 | 0.1063 | −368 | 28 | −103 | 84.49 |

*2.5. Theoretical Study.* Theoretical calculations were realized using density functional theory (DFT) by Gaussian 09W program with B3LYP/6-311G(d,p) orbital basis for atoms [22]. The molecular structures were optimized by Gauss View [23]. Energy of the highest occupied molecular orbital ($E_{HOMO}$), energy of the lowest unoccupied molecular orbital ($E_{LUMO}$), dipole moment ($\mu$), energy gap ($\Delta E$) between LUMO and HOMO, values of global hardness ($\rho$), and global softness ($\sigma$) were determined for each molecule.

## 3. Results and Discussion

*3.1. Potentiodynamic Polarization Measurements.* Polarization curves of steel in 1.0 M HCl solution in the absence and presence of different concentrations of Camphor thiosemicarbazone **(5)**, Carvone thiosemicarbazone **(6)**, and Pulegone thiosemicarbazone **(7)** are represented in Figure 2. Table 2 presents the electrochemical kinetic parameters such as corrosion current density ($i_{corr}$), corrosion potential ($E_{corr}$),

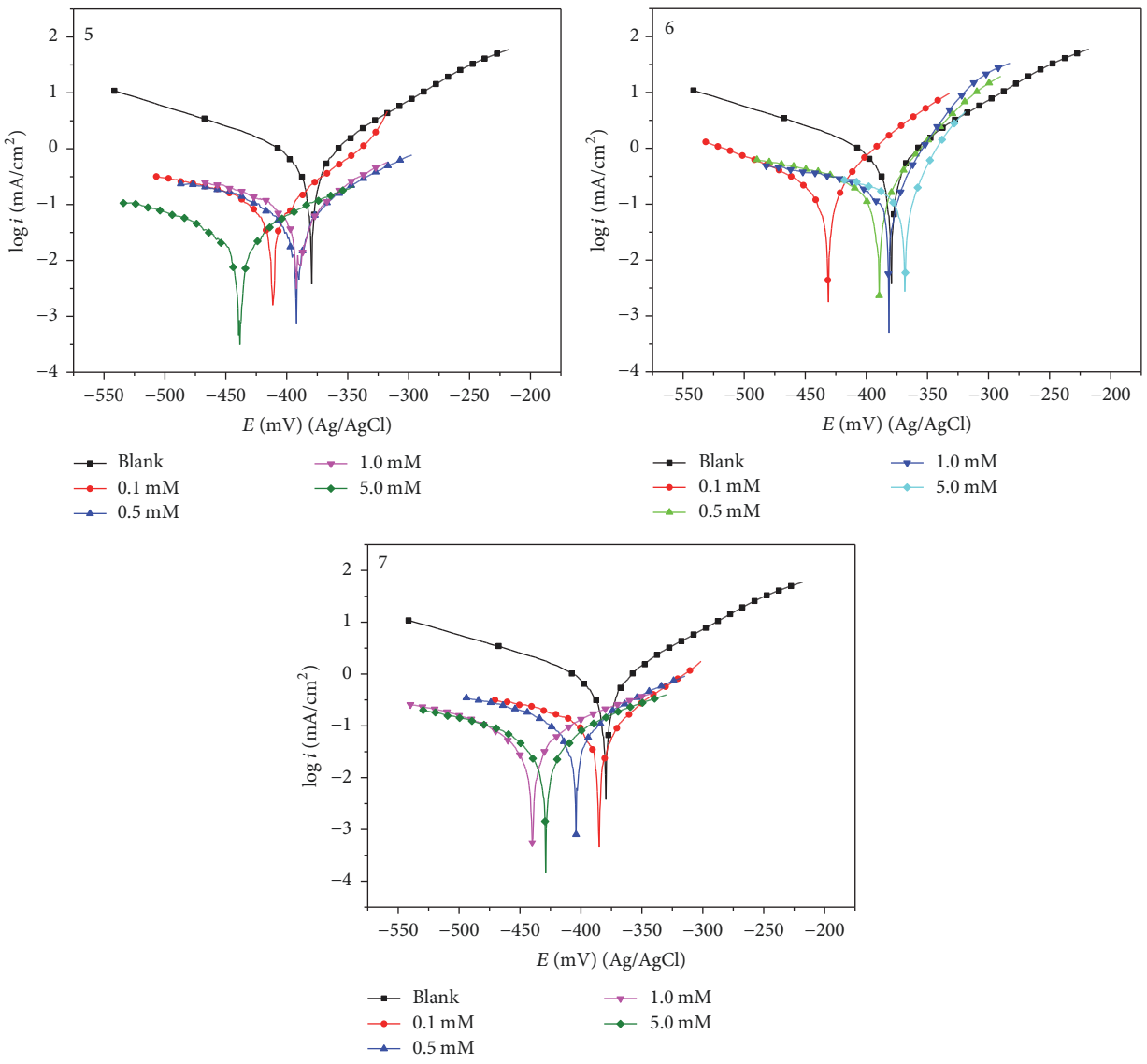


Figure 2: Polarization curves for steel in 1 M HCl before and after adding different concentrations of Camphor thiosemicarbazone (5), Carvone thiosemicarbazone (6), and Pulegone thiosemicarbazone (7).

cathodic and anodic Tafel slopes ($\beta c$ and $\beta a$), and inhibition efficiency ($\eta$%). These parameters were determined by extrapolation method of the experimental curves. The inhibition efficiency was calculated using the following equation:

$$\eta\ (\%) = \frac{i_{\text{corr}} - i'_{\text{corr}}\,(\text{inh})}{i_{\text{corr}}} * 100, \tag{1}$$

where $i_{\text{corr}}$ and $i'_{\text{corr}}$ are corrosion current densities for steel electrode without and with presence of inhibitors, respectively.

In order to study the kinetics of the anodic and cathodic reactions, the polarization curves were plotted. Figure 2 reveals that addition of inhibitors to acid solutions has an effect on both anodic and cathodic slopes of the Tafel plots, reducing the rate of anodic metal dissolution as well as retarding the cathodic hydrogen evolution reaction [24]. This indicates the mixed inhibitive nature of the inhibitors [18].

As shown in Table 2, the corrosion current density ($i_{\text{corr}}$) values decrease with increasing inhibitors concentrations as well as increase of inhibition efficiency, indicating that the adsorption of the inhibitors molecules on the surface of steel is impeded by blocking the reaction sites [25, 26]. It can be seen that the inhibition efficiency varies from 84.49% to 95.11% and shows the following order of inhibition: Camphor thiosemicarbazone (5), Carvone thiosemicarbazone (6), and Pulegone thiosemicarbazone (7), respectively, for the concentration of 5 mmol/L. In general, an inhibitor is an anodic or a cathodic type if the displacement in corrosion potential ($E_{\text{corr}}$) against the blank is higher than 85 mV [27]; while if the shift is less than 85 mV, it can be regarded as mixed type [28, 29]. In the present study, the maximum displacements were approximately 59 mV, 60 mV, and 51 mV towards cathodic

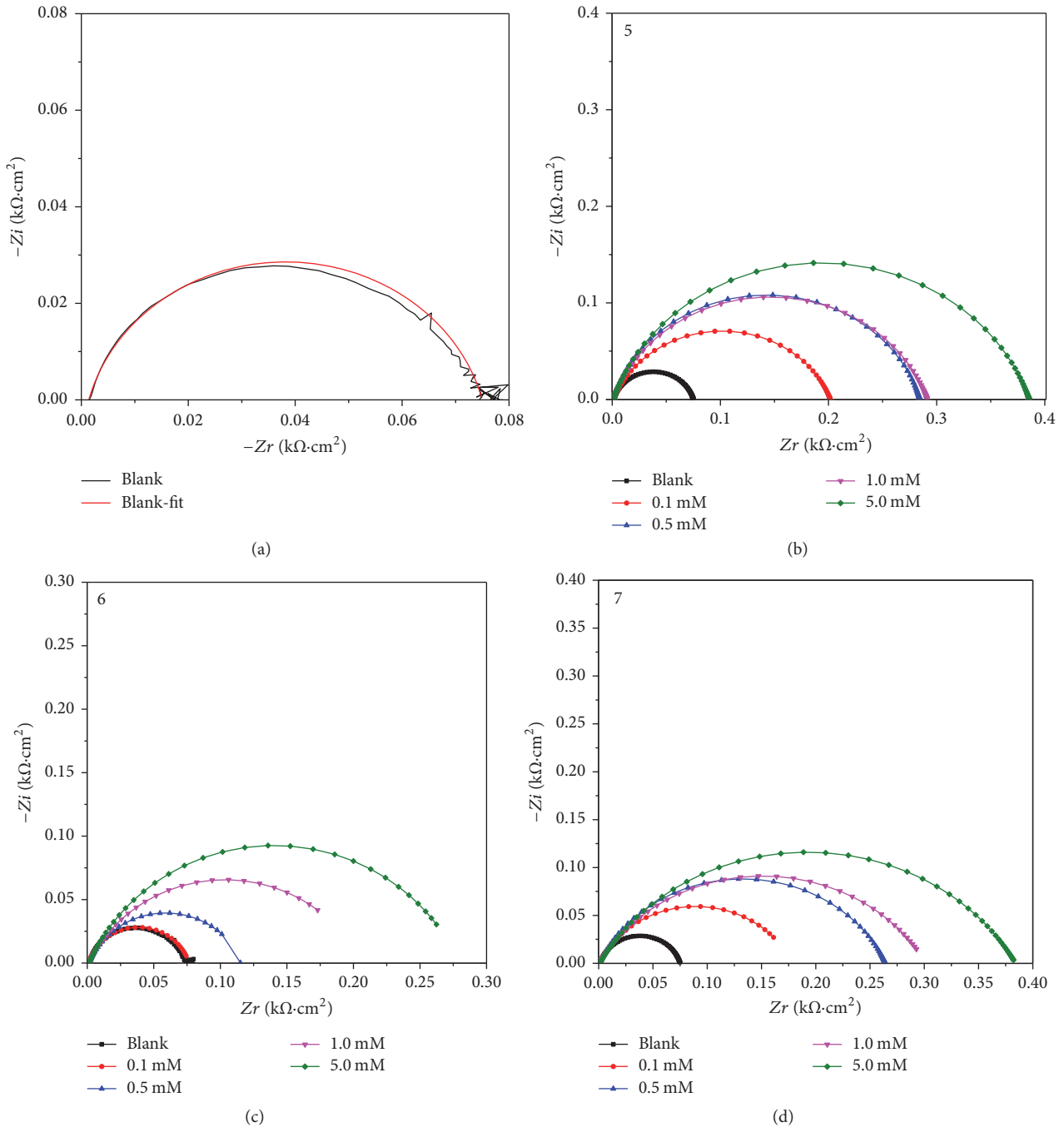


FIGURE 3: Nyquist plots of steel (a) in 1 M HCl (b) with different concentrations of Camphor thiosemicarbazone (c), with different concentrations of Carvone thiosemicarbazone (d), and with different concentrations of Pulegone thiosemicarbazone at 293 K.

curves for the three inhibitors, respectively, which indicates that the studied inhibitors should be considered as mixed type inhibitors with predominately cathodic effect.

*3.2. Electrochemical Impedance Spectroscopy (EIS).* Figures 3(a)–3(d) show the Nyquist plots of steel obtained in 1.0 M HCl solution in the absence and presence of various concentrations of Camphor thiosemicarbazone (5), Carvone thiosemicarbazone (6) and Pulegone thiosemicarbazone (7), respectively. Table 3 gives the impedance parameters such as charge transfer resistance ($R_{ct}$), electrolyte resistance ($R_e$), double layer capacitance ($C_{dl}$), constant phase elements ($Q_{dl}$), exponential value of CPE ($\alpha$), and inhibition efficiency ($\eta$%). The Nyquist plot of steel in the medium shows a single semicircular shape; this observation indicates that the corrosion of steel is controlled by a charge transfer process. The goodness of fit indicates a good correlation with the equivalent circuit model (Figure 3(a)) [30].

Table 3: Kinetic parameters derived from Nyquist plots of steel immersed in 1 M HCl with different concentrations of Camphor thiosemicarbazone (5), Carvone thiosemicarbazone (6), and Pulegone thiosemicarbazone (7) at 293 K.

| Inhibitors | $C$ (mmol/L) | $R_e$ ($\Omega\cdot cm^2$) | $R_{tc}$ ($\Omega\cdot cm^2$) | $C_{dc}$ ($\mu F/cm^2$) | $Q_{dl}$ ($\mu\Omega^{-1}cm^{-2}$ $S^{(\alpha-1)}$) | $\alpha$ | $\eta$ (%) |
|---|---|---|---|---|---|---|---|
| | Blank | 1.3 ± 0.1 | 58.3 ± 0.3 | 172.5 | 247.8 | 0.84 | --- |
| **(5)** | 0.1 | 2.29 ± 0.05 | 203.3 ± 0.7 | 49.5 | 123.6 | 0.78 | 71.32 |
| | 0.5 | 1.20 ± 0.07 | 296.5 ± 0.9 | 42.9 | 79.6 | 0.82 | 80.34 |
| | 1.0 | 1.7 ± 0.8 | 297.7 ± 1.3 | 42.8 | 90.3 | 0.80 | 80.42 |
| | 5.0 | 1.3 ± 0.3 | 439.0 ± 2.7 | 29.0 | 55.0 | 0.80 | 86.72 |
| **(6)** | 0.1 | 2.0 ± 0.2 | 178.8 ± 0.7 | 140.5 | 330.0 | 0.75 | 67.39 |
| | 0.5 | 0.64 ± 0.04 | 202.2 ± 0.9 | 124.3 | 175.8 | 0.75 | 71.17 |
| | 1.0 | 0.2 ± 0.3 | 349.4 ± 1.6 | 57.4 | 142.5 | 0.69 | 83.31 |
| | 5.0 | 0.9 ± 0.7 | 442.5 ± 2.1 | 89.9 | 178.7 | 0.70 | 86.82 |
| **(7)** | 0.1 | 0.99 ± 0.06 | 77.28 ± 0.3 | 146.7 | 341.9 | 0.81 | 24.56 |
| | 0.5 | 1.51 ± 0.01 | 114.9 ± 1.2 | 276.9 | 480.0 | 0.77 | 49.26 |
| | 1.0 | 3.05 ± 0.03 | 186.5 ± 0.9 | 213.2 | 386.6 | 0.72 | 68.74 |
| | 5.0 | 3.49 ± 0.04 | 267.5 ± 2.3 | 237.9 | 479.9 | 0.74 | 78.21 |

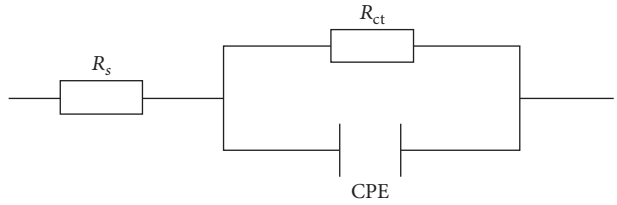


Figure 4: Equivalent electrical circuit of the interface of steel/HCl electrolyte.

It was observed that the diameters of semicircles in the Nyquist plots were influenced by the presence of inhibitors. The increase in diameter sizes with increasing inhibitor concentration may explain the influence of inhibitors on corrosion rate due to inhibition. The irregularity in the semicircle shape of Nyquist diagrams can be attributed to the inhomogeneity of the metal surface as a result of surface roughness or interface phenomena [31]. The Nyquist plots were analyzed by fitting experimental data to an equivalent electrical circuit shown in Figure 4.

It consists of electrolyte resistance ($R_e$), charge transfer resistance ($R_{ct}$), and one constant phase element (CPE). The CPE contains the component $Q_{dl}$ and the coefficient $\alpha$ that describes different physical phenomena such as surface roughness, inhibitor adsorption, and porous layer formation [32]. Thus, the capacitance can be deduced from the following relation:

$$C_{dl} = Q_{dl} \times \left(2\pi f_{max}\right)^{\alpha-1}. \quad (2)$$

It was observed that the values of $C_{dl}$ decreased with the increase of the concentration of different inhibitors from 0.1 to 5 mM (Table 3). This behavior confirms that the molecules of inhibitors are adsorbed on the steel surface. The decrease in $C_{dl}$ values may be considered in terms of Helmholtz model [33]:

$$C_{dl} = \frac{\varepsilon\varepsilon_0}{\delta} S, \quad (3)$$

where $\varepsilon$ is the dielectric constant of the medium, $\varepsilon_o$ the vacuum permittivity, $S$ the electrode area, and $\delta$ the thickness of the protective layer. As a matter of fact, the decrease in $C_{dl}$ values could be a result of decreasing local dielectric constant and/or increasing thickness of the electrical double layer. Table 3 explains clearly that the $R_{ct}$ values increased with the inhibitor concentration. This increase in charge transfer resistance can be related to the formation of a protective layer on the metal/solution interface [34].

From the outcome, it can be seen that inhibitors are efficient on steel in 1 M HCl solution. These higher inhibition efficiencies could be attributed to the presence in their molecular structures, of amino ($-NH_2$) and thioxo (=S) groups which are active centers of adsorption [23]. Indeed, the presence of these groups in the inhibitor molecules increases electron density on the adsorption centers leading to an easier electron transfer between functional group and the metal. The inhibition efficiencies of inhibitors **(5)**, **(6)**, and **(7)** at 5 mmol/L in 1 M hydrochloric acid are 86.72%, 86.82%, and 78.21%, respectively. The obtained results from the Nyquist curves are in good agreement with the polarization curves.

*3.3. Adsorption Isotherm.* The adsorption of the inhibitor on the metal surface can be provided by the adsorption isotherms which give precious information about the interaction between the organic molecules of the inhibitor and the metal surface [35]. The adsorption of organic inhibitor molecules from the aqueous solution can be regarded as a quasi-substitution process between the organic compounds in the aqueous phase [$org_{(sol)}$] and water molecules at the metal surface [$H_2O]_{ads}$ [36].

$$Org_{(sol)} + nH_2O_{(ads)} \longleftrightarrow Org_{(ads)} + nH_2O_{(sol)}, \quad (4)$$

Table 4: Langmuir adsorption parameters and free energy of adsorption of inhibitors on the steel surface at 293 K.

| Inhibitors | $K_{ads}$ | $\Delta G_{ads}$ (kJ/mol) | $R^2$ |
|---|---|---|---|
| (5) | 0.957 | −9.676 | 0.999 |
| (6) | 0.906 | −9.542 | 1.000 |
| (7) | 0.852 | −9.393 | 0.999 |

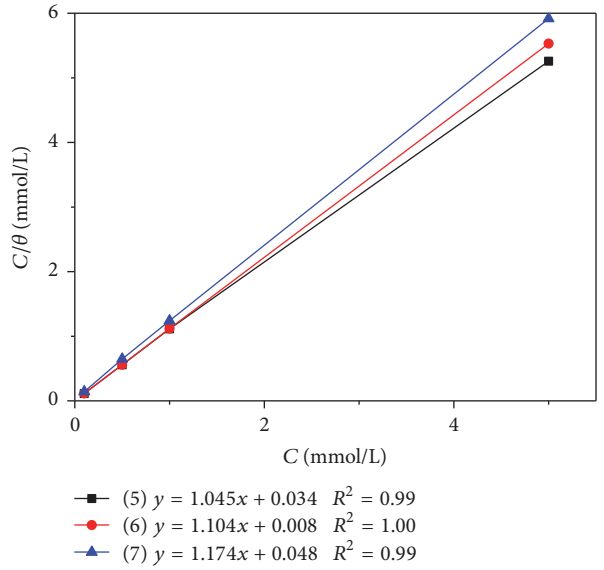


Figure 5: Langmuir adsorption plot for steel in 1 M HCl containing different inhibitors at 293 K.

where $Org_{(sol)}$ and $Org_{(ads)}$ are the organic species dissolved in the aqueous solution and adsorbed onto the metallic surface, respectively. $H_2O_{(ads)}$ are water molecules adsorbed on the metallic surface and $n$ is the size ratio representing the number of water molecules replaced by one organic adsorbate. In order to obtain the isotherm that fits best, the surface coverage was derived from the equation:

$$\theta = \frac{i_{corr} - i_{corr}^{inh}}{i_{corr}}, \quad (5)$$

where $i_{corr}^{inh}$ and $i_{corr}$ are the current densities of steel with and without inhibitor, respectively. In the present work, several adsorption isotherms (Langmuir–Freundlich–Temkin) have been tested in order to determine the best fitting model. The correlation coefficients between surface coverage ($\theta$) and the amount of inhibitors in the corroding medium were compared; the adsorption data fitted well to the three models but gave a better fit to the Langmuir model, as it was evidenced by the higher value of $R^2$: 0.999, 1, and 0.999 for Camphor thiosemicarbazone **(5)**, Carvone thiosemicarbazone **(6)**, and Pulegone thiosemicarbazone **(7)**, respectively.

The Langmuir equation was developed under the assumptions that adsorption is monolayer, all active sites have uniform distribution of energy level, and there is no interaction between adjacent adsorbed molecules [37].

So, the Langmuir adsorption can be given as

$$\frac{C_{inh}}{\theta} = \frac{1}{K_{ads}} + C_{inh}, \quad (6)$$

where $\theta$ is the surface coverage, $C_{inh}$ is the concentration of the inhibitor, and $K_{ads}$ is the equilibrium constant of the adsorption process. As shown in Figure 5, the plot of $C/\theta$ versus $C$ for different inhibitors at 293 K gave straight lines which suggested a monolayer adsorption of inhibitors species at the metal surface and no interaction between the adsorbed molecules [38].

The free energy values $\Delta G_{ads}$ of inhibitors adsorption on steel surface were calculated using (6):

$$\Delta G_{ads} = -RT \ln\left(55.5 K_{ads}\right), \quad (7)$$

where $R$ is the gas constant, $T$ is the absolute temperature, and 55.5 is the concentration of water in the solution in mol·L$^{-1}$. The negative values of $\Delta G_{ads}$ (Table 4) indicate the spontaneous adsorption of inhibitors on the steel surface [29]. Generally, the energy values of $\Delta G^{\circ}_{ads}$ around −20 kJ mol$^{-1}$ or less negative are associated with an electrostatic interaction between charged inhibitor molecules and charged metal surface (physisorption); those around −40 kJ mol$^{-1}$ or more negative involve charge sharing or transfer from the inhibitor molecules to the metal surface to form a coordinate type bond (Chemisorption) [39]. As can be seen in Table 4, the $\Delta G^{\circ}_{ads}$ values are around −9.5 kJ/mol, indicating that the adsorption of inhibitors at 293 K in 1 M HCl solution was a physisorption interaction.

*3.4. Temperature Effect and Thermodynamic Parameters.* Temperature has a significant effect on the corrosion phenomenon. It influences the corrosion rate of metal and

Table 5: The influence of temperature on the electrochemical parameters for steel electrode immersed in 1 M HCl and 1 M HCl + 5 mmol/L of inhibitors.

| | $T$ (K) | $i_{corr}$ (mA/cm$^2$) | $E_{corr}$/mV (Ag/AgCl) | $\beta a$ (mV/dec) | $\beta c$ (mV/dec) | $\eta$ (%) |
|---|---|---|---|---|---|---|
| Blank | 293 | 0.682 | −379 | 77 | −142 | – |
| | 303 | 0.896 | −376 | 84 | −181 | – |
| | 313 | 1.246 | −388 | 87 | −201 | – |
| | 323 | 2.677 | −401 | 133 | −121 | – |
| (5) | 293 | 0.033 | −438 | 116 | −170 | 95.11 |
| | 303 | 0.049 | −409 | 73 | −135 | 94.47 |
| | 313 | 0.026 | −449 | 99 | −223 | 97.87 |
| | 323 | 0.177 | −446 | 70 | −80 | 93.35 |
| **(6)** | 293 | 0.065 | −428 | 126 | −204 | 90.41 |
| | 303 | 0.066 | −443 | 119 | −230 | 92.64 |
| | 313 | 0.077 | −430 | 72 | −95 | 93.78 |
| | 323 | 0.187 | −441 | 106 | −159 | 92.98 |
| **(7)** | 293 | 0.106 | −368 | 28 | −103 | 84.94 |
| | 303 | 0.065 | −424 | 100 | −190 | 92.69 |
| | 313 | 0.066 | −402 | 36 | −95 | 94.65 |
| | 323 | 0.139 | −421 | 70 | −124 | 94.78 |

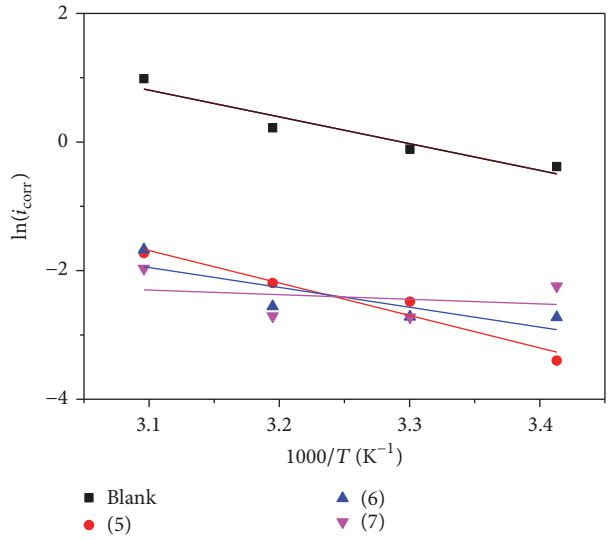


Figure 6: Arrhenius plots of ln($i_{corr}$) versus $1/T$ (K$^{-1}$) in 1 M HCl in the absence and presence of 5 mM of inhibitors.

modifies the inhibition characteristics as the inhibitor itself may undergo decomposition and/or rearrangements [40]. In order to evaluate the thermodynamic parameters for the inhibition and the adsorption process, polarization experiments were conducted in the range from 293 to 323 K in the absence and presence of 5 mmol/L of inhibitors. The corresponding data are given in Table 5. Increasing the temperature shifts corrosion potentials to low values. This leads to the increase of inhibition efficiency and suggests that the inhibitor molecules act by adsorption on the steel surface in the acid medium which is a characteristic of chemisorption [4]. Examination of data in Table 5 reveals that Camphor thiosemicarbazone **(5)** exhibits better stability with the temperature evolution.

The corrosion reaction can be studied as an Arrhenius-type process using the following relation:

$$\ln i_{corr} = \ln A - \frac{E_a}{R \cdot T}, \tag{8}$$

where $i_{corr}$ is the corrosion current density of steel, $E_a$ is the apparent activation energy, $A$ is the Arrhenius preexponential constant, $R$ is the universal gas constant, and $T$ is the absolute temperature. An Arrhenius plot of current density logarithm versus $1/T$ produces a straight line with a slope of $E_a/R$, as shown in Figure 6. Analysis of activation parameters in the absence and presence of inhibitors gives an insight into the inhibitor adsorption mechanism. It can be seen from

Table 6: The values of thermodynamic parameters for steel in 1 M HCl in the absence and the presence of Camphor thiosemicarbazone (5), Carvone thiosemicarbazone (6), and Pulegone thiosemicarbazone (7), respectively.

| | Blank | (5) | (6) | (7) |
|---|---|---|---|---|
| $\Delta H_a^*$ (kJ·mol$^{-1}$) | 32.02 | 39.41 | 23.13 | 3.40 |
| $\Delta S$ (J·mol$^{-1}$·K$^{-1}$) | −139.59 | −137.42 | −190.09 | −254.16 |
| $Ea$ (kJ·mol$^{-1}$) | 34.57 | 41.96 | 25.68 | 5.95 |
| $Ea - \Delta H$ | 2.56 | 2.56 | 2.56 | 2.56 |

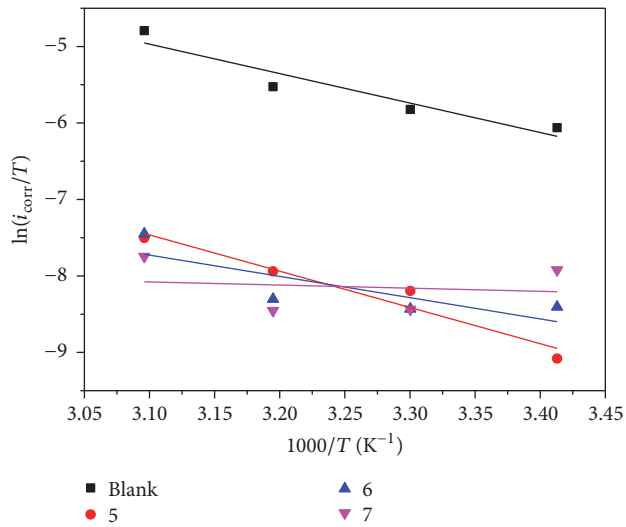


Figure 7: Transition-state plots of $\ln(i_{corr}/T)$ versus $1/T$ (K$^{-1}$) in 1 M HCl in the absence and presence of 5 mM of inhibitors.

Table 6 that the lower activation energy values for the corrosion process, in 1 M HCl and in the presence of 5 mmol/L of the inhibitors, indicate a chemisorption process of the inhibitors.

Activation parameters, such as enthalpy and entropy of corrosion process, may be evaluated from the effect of temperature. An alternative formulation of Arrhenius equation is

$$i_{corr} = \frac{TR}{hN} \exp\left(\frac{\Delta S_a^*}{R}\right) \exp\left(-\frac{\Delta H_a^*}{RT}\right), \quad (9)$$

where $h$ is Planck's constant, $N$ is Avogadro's number, $\Delta S_a^*$ is the entropy of activation, $\Delta H_a^*$ is the enthalpy of activation, $T$ is the absolute temperature, and $R$ is the universal gas constant.

Figure 7 shows the variation of $\ln(i_{corr}/T)$ against $1000/T$ in the absence and presence of inhibitors. Straight lines are obtained with a slope of $(-\Delta H_a^*/RT)$ and an intercept of $(\ln(R/hN) + \Delta S_a^*/R)$ from which the values of $\Delta H_a^*$ and $\Delta S_a^*$ are calculated, respectively.

The $\Delta H_a^*$ values are positive for all inhibitors, which suggest an endothermic adsorption process of inhibitors molecules onto metal surface. The negative values of $\Delta S_a^*$ accompanied by a reduction in entropy indicate that the inhibitor molecules were orderly adsorbed onto the steel surface [35, 41].

### 3.5. Surface Investigation

*3.5.1. SEM Analysis.* Steel surface analysis was carried out using SEM after 2 h immersion (Figure 8). The morphology of steel after immersion in 1 M HCl solution in the absence of inhibitors is very rough and strongly damaged due to corrosion attack of the acid (Figure 8(a)) [4]. The SEM images of the surface after addition of 5 mmol/L of inhibitors indicate the presence of a protective film on the steel surface; as it is revealed in Figures 8(b), 8(c), and 8(d), no damage is observed. A close examination of Figure 8 explains clearly that the surface of steel is best protected with inhibitors (6) and (7) with a less film [42]. This higher inhibition efficiency of the studied inhibitors is likely ascribable to a strong bonding between ($-NH_2$) and (=S) groups in the molecular structures of the inhibitors and the metal surface, blocking the active centers of adsorption.

*3.5.2. EDX Analysis.* Energy dispersive X-ray spectroscopy analysis was carried out in order to obtain information about the composition of the steel sample surface, without and with inhibitors in hydrochloric acid 1 M. Surface analysis was performed after two hours of immersion in the corrosive solution containing 5 mmol/L of inhibitors at the highest inhibition efficiency (Figure 9). The results of Atomic (At%) and Weight (Wt%) percentages of elements obtained from EDX analysis of steel in the absence and presence of 5 mmol/L of inhibitors are shown in Table 7.

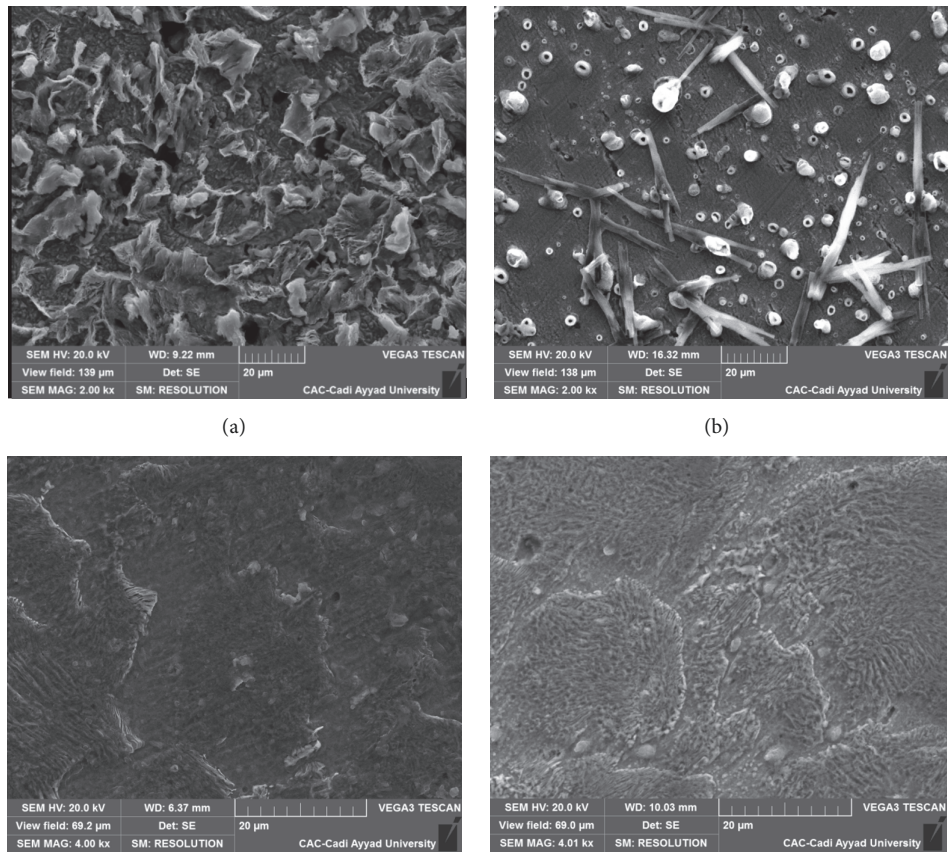


FIGURE 8: SEM images of steel in 1 M HCl solution after 2 h of immersion at 293 K; (a) steel in 1 M HCl (Blank), (b) steel in 1 M HCl in the presence of inhibitor (5), (c) steel in 1 M HCl in the presence of inhibitor (6), and (d) steel in 1 M HCl in the presence of inhibitor (7).

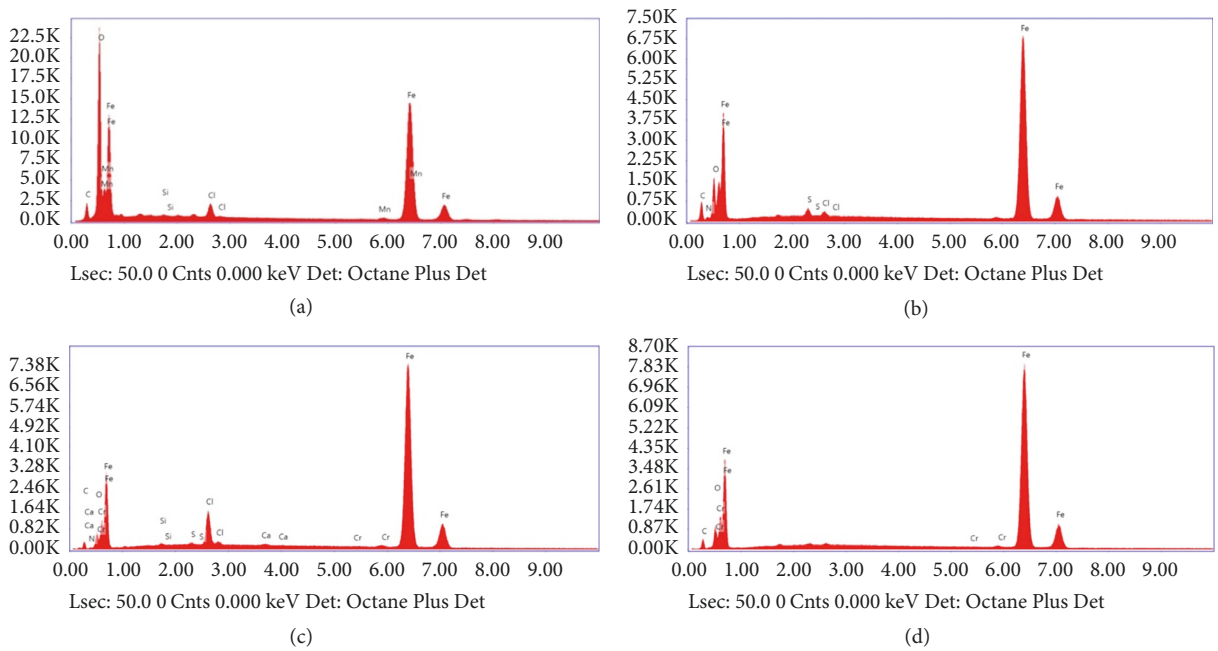


FIGURE 9: EDX spectra of steel specimens in the absence and presence of 5 mmol/L inhibitors (a) steel in 1 M HCl (Blank), (b) steel in 1 M HCl in the presence of inhibitor (5), (c) steel in 1 M HCl in the presence of inhibitor (6), and (d) steel in 1 M HCl in the presence of inhibitor (7) after 2 h of immersion at 293 K.

Table 7: Atomic (At) and Weight (Wt) percentages of elements obtained from EDX spectra of steel in 1 M HCl with and without inhibitors.

| Element | Case a (blank) | | Case b (5) | | Case c (6) | | Case d (7) | |
|---|---|---|---|---|---|---|---|---|
| | Wt% | At% | Wt% | At% | Wt% | At% | Wt% | At% |
| Fe | 93.15 | 80.73 | 80.25 | 50.62 | 87.04 | 68.19 | 89.16 | 66.54 |
| C | 1.28 | 5.15 | 9.07 | 26.61 | 4.37 | 15.94 | 6.50 | 22.54 |
| O | 3.94 | 11.92 | 7.22 | 15.91 | 3.18 | 8.68 | 4.12 | 10.74 |
| N | - | - | 2.20 | 5.54 | 0.26 | 0.80 | - | - |
| Cl | 0.49 | 0.67 | - | - | - | - | - | - |
| Si | - | - | - | - | - | - | - | - |

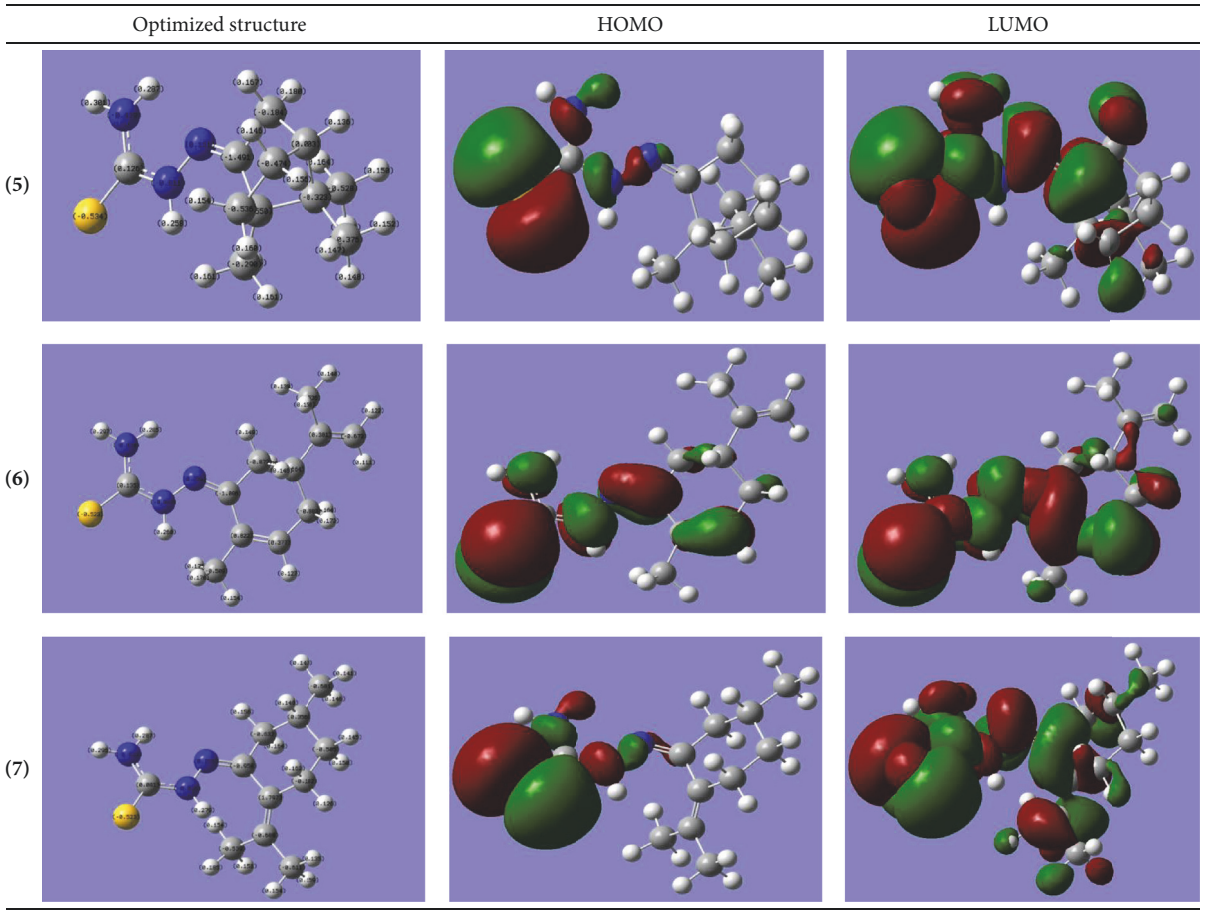


Figure 10: Calculated energies of HOMO and LUMO molecular orbitals and optimized structure of the studied molecules using B3LYP/6-311G (d, p).

Examination of Figure 9 reveals that the presence of inhibitors clearly decreased the O and Cl peaks while the peak of C increased. The peak of O is very high in hydrochloride solution due to the formation of iron oxide on the metal surface [43]. It is totally understandable that the presence of the inhibitors protects the surface without corrosion products, as shown in Figure 9 and confirmed by EDX data [44]. These results testify the good adsorption of inhibitor molecules on the steel surface forming a protective film.

*3.6. Quantum Chemical Calculation.* Quantum chemical calculation is a powerful tool to study the fundamental of corrosion inhibition in order to investigate the adsorption and the inhibition mechanism of studied inhibitor molecules [45]. Figure 10 shows calculated energy of highest occupied molecular orbital ($E_{HOMO}$) and lowest unoccupied molecular orbital ($E_{LUMO}$) (called the frontier orbitals) and optimized structure of the studied inhibitors. $E_{HOMO}$ and $E_{LUMO}$ determinate the way the molecule interacts with other species [7, 46]. To describe the polarity, we use the dipole moment of the molecule ($\mu$). Dipole moment is the polarity measurement of a polar covalent bond. The difference between the HOMO and LUMO energies for the molecules was calculated.

$$\Delta E = \left(E_{LUMO} - E_{HOMO}\right). \quad (10)$$

Table 8: Quantum chemical calculation parameters of Camphor thiosemicarbazone (5), Carvone thiosemicarbazone (6), and Pulegone thiosemicarbazone (7), respectively.

| Inhibitors | Dipole moment ($\mu$) (Debye) | $E_{HOMO}$ (Hartree) | $E_{LUMO}$ (Hartree) | $\Delta E$ (Hartree) | $\rho$ (Hartree) | $\sigma$ (Hartree) |
|---|---|---|---|---|---|---|
| (5) | 6.5232 | −0.20980 | −0.03661 | 0.17319 | 0.08659 | 11.548 |
| (6) | 5.9892 | −0.20993 | −0.04413 | 0.1658 | 0.0829 | 12.063 |
| (7) | 5.8051 | −0.21308 | −0.06456 | 0.14852 | 0.07426 | 13.46 |

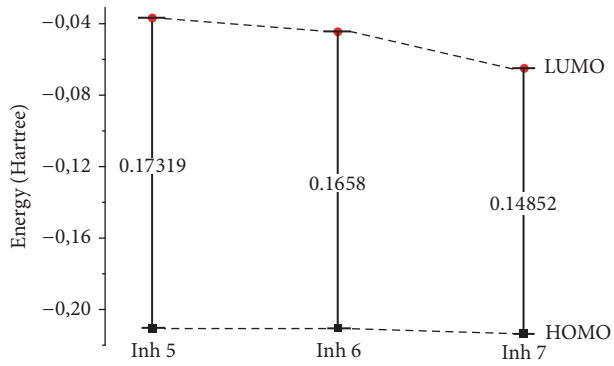


Figure 11: Correlation diagram of frontier molecular orbitals for the investigated inhibitors and their calculated $\Delta E$ (Hartree).

The values of global hardness ($\rho$) and global softness ($\sigma$) were calculated, according to Koopman's theory, from the values of $E_{HOMO}$ and $E_{LUMO}$ using the following equations [39, 47]:

$$\rho\,(\text{eV}) = \frac{(I - A)}{2} = \frac{(E_{LUMO} - E_{HOMO})}{2} = \frac{\Delta E}{2}, \qquad \sigma = \frac{1}{\rho}. \tag{11}$$

The values of calculated quantum chemical parameters such as $\mu$, $E_{HOMO}$, $E_{LUMO}$, $\Delta E$ (Hartree), $\rho$ (Hartree), and $\sigma$ (Hartree) of the studied inhibitors are listed in Table 8.

The increase in $E_{HOMO}$ values facilitates the adsorption of inhibitor by influencing the transport process through the adsorbed layer. For low values of $E_{LUMO}$, the molecule would accept electrons [7]. Low absolute values of the energy band gap give high inhibition efficiency because the energy to remove an electron from the last occupied orbital will be lower [48]. The dipole moment is the quantum parameter describing the polarity and the reactivity of molecules [30]. Large dipole moment will involve the accumulation of inhibitor in the surface layer, hence inhibition efficiency increase [22]. Global hardness ($\rho$) and global softness ($\sigma$) parameters are global chemical descriptors measuring molecular stability and reactivity.

In the present study, the values of quantum chemical parameters are given in Table 8. The higher value of dipole moment $\mu$ (6.5232 D) of inhibitor (5) compared to other molecules indicates its high reactivity and polarity so that it can easily donate electrons to establish strong d$\pi$-p$\pi$ bonds in order to form a protective surface film which is correlated to $\eta$ (%) [49]. In line with this, the positive sign of this parameter suggests the physical adsorption mechanism which is consistent with results obtained from adsorption studies. HOMO describes electron donor, while the LUMO is considered for electron acceptor [50]. The values of HOMO follow the order **(7)** < **(6)** < **(5)** which is in accordance with inhibition efficiency. Table 8 shows that the $E_{HOMO}$ is higher for inhibitor (5) compared to other molecules having higher inhibition efficiency. The results obtained in Figure 11 exhibit clearly that the energy band gap $\Delta E$ follows the order: **(7)** < **(6)** < **(5)** which is opposite to the order of $\eta$ (%). The same conclusion can be drawn from the values of $E_{LUMO}$.

The values of global hardness ($\rho$) and global softness ($\sigma$) explain the magnitude of electron transfer from inhibitor to metal. The inhibition efficiency increases with decreasing hardness and increasing softness of the inhibitor. In our study, the values of $\rho$ and $\sigma$ converse with the order of inhibition efficiency. Moreover, no relationship has been found between the global hardness ($\rho$), global softness ($\sigma$), energy gaps values, and inhibition efficiencies [48]. Besides, the experimental results showed that the molecule **(5)** acts efficiently at 293 K, whereas the molecule **(7)** presents a good performance at 323 K.

The studied molecules contain the functional groups such as =S, $-NH_2$, N–N=, and NH which are known in several research papers for their highest inhibition efficiency. The amine function can form coordination bonds between the unshared electron pair of N atom and the unoccupied d electronic of Fe [51]. The adsorption of functional groups containing the sulfur atom could be realized by formation of links between the d-orbital of iron and heteroatom, leading to water molecules displacement on steel surface. The electron density distribution of HOMO and LUMO of the studied inhibitors was shown in Figure 10. It is expected that the electron density of HOMO and LUMO is localized principally on the S and N atoms, these assumed to be strongly adsorbed on the metal surface [52].

## 4. Conclusion

The Monoterpenic Thiosemicarbazones (5–7) are efficient inhibitors for the steel corrosion in 1 M HCl with a maximum efficiency of 95%. The corrosion process was inhibited by adsorption of these molecules on the steel surface. The negative values of $\Delta G_{ads}$ reflect the spontaneity of the adsorption of the inhibitor and the positive sign of activation energy shows an endothermic nature of the reaction. Lower values of free energy show that the inhibitors are physically adsorbed at lower temperature, while the decrease in activation energy favored a chemisorption process as temperature increases. The adsorption of these inhibitors follows the Langmuir adsorption isotherm. The inhibition efficiency of these inhibitors towards corrosion depends mainly on their structure. SEM/EDX studies reveal that the corrosion of mild steel in 1 M HCl was diminished by the addition of inhibitors. The correlation between the electronic-structural properties of the studied molecules and their inhibition efficiencies provided by electrochemical study is evidenced by the application of DFT.

## Conflicts of Interest

The authors declare that they have no conflicts of interest.

## Acknowledgments

The authors are grateful to the Center of Analyses and Characterization (CAC) at the Cady Ayyad University, Morocco. They also wish to thank Dr. A. JARID for his valuable help and comments.

## References

[1] S. A. Abd El–Maksoud, "The effect of organic compounds on the electrochemical behaviour of steel in acidic media. A review," *International Journal of Electrochemical Science*, vol. 3, pp. 528–555, 2008.

[2] J. Saranya, P. Sounthari, K. Parameswari, and S. Chitra, "Acenaphtho[1,2-b]quinoxaline and acenaphtho[1,2-b]pyrazine as corrosion inhibitors for mild steel in acid medium," *Measurement*, vol. 77, pp. 175–185, 2016.

[3] F. Bentiss, M. Lagrenee, M. Traisnel, and J. C. Hornez, "The corrosion inhibition of mild steel in acidic media by a new triazole derivative," *Corrosion Science*, vol. 41, no. 4, pp. 789–803, 1999.

[4] M. A. Hegazy, H. M. Ahmed, and A. S. El-Tabei, "Investigation of the inhibitive effect of p-substituted 4-(N,N,N-dimethyldodecylammonium bromide)benzylidene-benzene-2-yl-amine on corrosion of carbon steel pipelines in acidic medium," *Corrosion Science*, vol. 53, no. 2, pp. 671–678, 2011.

[5] B. E. A. Rani and B. B. J. Basu, "Green inhibitors for corrosion protection of metals and alloys: an overview," *International Journal of Corrosion*, vol. 2012, Article ID 380217, 15 pages, 2012.

[6] A. Singh, E. E. Ebenso, and M. A. Quraishi, "Corrosion inhibition of carbon steel in HCl solution by some plant extracts," *International Journal of Corrosion*, vol. 2012, Article ID 897430, 20 pages, 2012.

[7] G. Gece, "The use of quantum chemical methods in corrosion inhibitor studies," *Corrosion Science*, vol. 50, no. 11, pp. 2981–2992, 2008.

[8] T. Arslan, F. Kandemirli, E. E. Ebenso, I. Love, and H. Alemu, "Quantum chemical studies on the corrosion inhibition of some sulphonamides on mild steel in acidic medium," *Corrosion Science*, vol. 51, no. 1, pp. 35–47, 2009.

[9] S. K. Shukla and M. A. Quraishi, "Cefotaxime sodium: a new and efficient corrosion inhibitor for mild steel in hydrochloric acid solution," *Corrosion Science*, vol. 51, no. 5, pp. 1007–1011, 2009.

[10] N. K. Gupta, C. Verma, M. A. Quraishi, and A. K. Mukherjee, "Schiff's bases derived from l-lysine and aromatic aldehydes as green corrosion inhibitors for mild steel: Experimental and theoretical studies," *Journal of Molecular Liquids*, vol. 215, pp. 47–57, 2016.

[11] H. Lgaz, K. Subrahmanya Bhat, R. Salghi et al., "Insights into corrosion inhibition behavior of three chalcone derivatives for mild steel in hydrochloric acid solution," *Journal of Molecular Liquids*, vol. 238, pp. 71–83, 2017.

[12] R. Kumar, O. S. Yadav, and G. Singh, "Electrochemical and surface characterization of a new eco-friendly corrosion inhibitor for mild steel in acidic media: A cumulative study," *Journal of Molecular Liquids*, vol. 237, pp. 413–427, 2017.

[13] V. Srivastava, J. Haque, C. Verma et al., "Amino acid based imidazolium zwitterions as novel and green corrosion inhibitors for mild steel: Experimental, DFT and MD studies," *Journal of Molecular Liquids*, vol. 244, pp. 340–352, 2017.

[14] G. M. Pinto, J. Nayak, and A. N. Shetty, "Corrosion inhibition of 6061 Al-15 vol. pct. SiC(p) composite and its base alloy in a mixture of sulphuric acid and hydrochloric acid by 4-(N,N-dimethyl amino) benzaldehyde thiosemicarbazone," *Materials Chemistry and Physics*, vol. 125, no. 3, pp. 628–640, 2011.

[15] K. F. Khaled, "Electrochemical behavior of nickel in nitric acid and its corrosion inhibition using some thiosemicarbazone derivatives," *Electrochimica Acta*, vol. 55, no. 19, pp. 5375–5383, 2010.

[16] N. Karakus and K. Sayin, "The investigation of corrosion inhibition efficiency on some benzaldehyde thiosemicarbazones and their thiole tautomers: Computational study," *Journal of the Taiwan Institute of Chemical Engineers*, vol. 48, pp. 95–102, 2015.

[17] B. I. Ita and O. E. Offiong, "The study of the inhibitory properties of benzoin, benzil, benzoin-(4-phenylthiosemicarbazone) and benzil-(4-phenylthiosemicarbazone) on the corrosion of mild steel in hydrochloric acid," *Materials Chemistry and Physics*, vol. 70, no. 3, pp. 330–335, 2001.

[18] C. M. Goulart, A. Esteves-Souza, C. A. Martinez-Huitle, C. J. F. Rodrigues, M. A. M. Maciel, and A. Echevarria, "Experimental and theoretical evaluation of semicarbazones and thiosemicarbazones as organic corrosion inhibitors," *Corrosion Science*, vol. 67, pp. 281–291, 2013.

[19] L. Somogyi, "Unexpected transformations of camphor (thio)semicarbazones under acetylating conditions," *Liebigs Annalen der Chemie*, vol. 1991, no. 12, pp. 1267–1271, 1991.

[20] B. Glinma, S. D. S. Kpoviessi, R. H. Fatondji et al., "Synthesis, characterization and anti-trypanosomal activity of R-(-)carvone and arylketones-thiosemi carbazones and toxicity against Artemia salina leach," *Journal of Applied Pharmaceutical Science*, vol. 1, no. 8, pp. 65–70, 2011.

[21] C. C. García, B. N. Brousse, M. J. Carlucci et al., "Inhibitory effect of thiosemicarbazone derivatives on Junin virus replication in vitro," *Antiviral Chemistry & Chemotherapy*, vol. 14, no. 2, pp. 99–105, 2003.

[22] E. Gutiérrez, J. A. RodrÃguez, J. Cruz-Borbolla, J. G. Alvarado-RodrÃguez, and P. Thangarasu, "Development of a predictive model for corrosion inhibition of carbon steel by imidazole and benzimidazole derivatives," *Corrosion Science*, vol. 108, pp. 23–35, 2016.

[23] A. Döner, R. Solmaz, M. Özcan, and G. Kardaş, "Experimental and theoretical studies of thiazoles as corrosion inhibitors for mild steel in sulphuric acid solution," *Corrosion Science*, vol. 53, no. 9, pp. 2902–2913, 2011.

[24] M. Prabakaran, S.-H. Kim, V. Hemapriya, M. Gopiraman, I. S. Kim, and I.-M. Chung, "Rhus verniciflua as a green corrosion inhibitor for mild steel in 1 M $H_2SO_4$," *RSC Advances*, vol. 6, no. 62, pp. 57144–57153, 2016.

[25] K. Boumhara, M. Tabyaoui, C. Jama, and F. Bentiss, "Artemisia Mesatlantica essential oil as green inhibitor for carbon steel corrosion in 1M HCl solution: Electrochemical and XPS investigations," *Journal of Industrial and Engineering Chemistry*, vol. 29, pp. 146–155, 2015.

[26] M. Prabakaran, S.-H. Kim, K. Kalaiselvi, V. Hemapriya, and I.-M. Chung, "Highly efficient *Ligularia fischeri* green extract for the protection against corrosion of mild steel in acidic medium: electrochemical and spectroscopic investigations," *Journal of the Taiwan Institute of Chemical Engineers*, vol. 59, pp. 553–562, 2016.

[27] R. K. Pathak and P. Mishra, "Drugs as corrosion inhibitors: a review," *International Journal of Science and Research*, vol. 5, no. 4, pp. 671–677, 2016.

[28] X. Lei, H. Wang, Y. Feng et al., "Synthesis, evaluation and thermodynamics of a 1H-benzo-imidazole phenanthroline derivative as a novel inhibitor for mild steel against acidic corrosion," *RSC Advances*, vol. 5, no. 120, pp. 99084–99094, 2015.

[29] R. Idouhli, A. Abouelfida, A. Benyaich, and A. Aityoub, "Cuminum Cyminum Extract- A Green Corrosion Inhibitor of S300 Steel in 1 M HCl," *Chemical and Process Engineering*, vol. 44, no. 0, pp. 16–25, 2016.

[30] E. Ituen, O. Akaranta, and A. James, "Green anticorrosive oilfield chemicals from 5-hydroxytryptophan and synergistic additives for X80 steel surface protection in acidic well treatment fluids," *Journal of Molecular Liquids*, vol. 224, pp. 408–419, 2016.

[31] L. Li, X. Zhang, J. Lei, J. He, S. Zhang, and F. Pan, "Adsorption and corrosion inhibition of Osmanthus fragran leaves extract on carbon steel," *Corrosion Science*, vol. 63, pp. 82–90, 2012.

[32] P. Muthukrishnan, P. Prakash, B. Jeyaprabha, and K. Shankar, "Stigmasterol extracted from Ficus hispida leaves as a green inhibitor for the mild steel corrosion in 1M HCl solution," *Arabian Journal of Chemistry*, 2015.

[33] A. Khadraoui, A. Khelifa, M. Hadjmeliani et al., "Extraction, characterization and anti-corrosion activity of Mentha pulegium oil: Weight loss, electrochemical, thermodynamic and surface studies," *Journal of Molecular Liquids*, vol. 216, pp. 724–731, 2016.

[34] N. El Hamdani, R. Fdil, M. Tourabi, C. Jama, and F. Bentiss, "Alkaloids extract of Retama monosperma (L.) Boiss. seeds used as novel eco-friendly inhibitor for carbon steel corrosion in 1 M HCl solution: Electrochemical and surface studies," *Applied Surface Science*, vol. 357, pp. 1294–1305, 2015.

[35] E. A. Noor and A. H. Al-Moubaraki, "Thermodynamic study of metal corrosion and inhibitor adsorption processes in mild steel/1-methyl-4[4′(-X)-styryl pyridinium iodides/hydrochloric acid systems," *Materials Chemistry and Physics*, vol. 110, no. 1, pp. 145–154, 2008.

[36] I. Ahamad, R. Prasad, and M. A. Quraishi, "Thermodynamic, electrochemical and quantum chemical investigation of some Schiff bases as corrosion inhibitors for mild steel in hydrochloric acid solutions," *Corrosion Science*, vol. 52, no. 3, pp. 933–942, 2010.

[37] A. Adewuyi, A. Göpfert, and T. Wolff, "Succinyl amide gemini surfactant from Adenopus breviflorus seed oil: A potential corrosion inhibitor of mild steel in acidic medium," *Industrial Crops and Products*, vol. 52, pp. 439–449, 2014.

[38] P. Muthukrishnan, B. Jeyaprabha, and P. Prakash, "Adsorption and corrosion inhibiting behavior of Lannea coromandelica leaf extract on mild steel corrosion," *Arabian Journal of Chemistry*, vol. 10, pp. S2343–S2354, 2017.

[39] D. Jeroundi, H. Elmsellem, S. Chakroune et al., "Physicochemical study and corrosion inhibition potential of dithiolo[4,5-b][1,4]dithiepine for mild steel in acidic medium," *Journal of Materials and Environmental Science*, vol. 7, no. 11, pp. 4024–4035, 2016.

[40] J. Aljourani, K. Raeissi, and M. A. Golozar, "Benzimidazole and its derivatives as corrosion inhibitors for mild steel in 1M HCl solution," *Corrosion Science*, vol. 51, no. 8, pp. 1836–1843, 2009.

[41] G. Mu, X. Li, and G. Liu, "Synergistic inhibition between tween 60 and NaCl on the corrosion of cold rolled steel in 0.5 M sulfuric acid," *Corrosion Science*, vol. 47, no. 8, pp. 1932–1952, 2005.

[42] P. Singh, V. Srivastava, and M. A. Quraishi, "Novel quinoline derivatives as green corrosion inhibitors for mild steel in acidic medium: electrochemical, SEM, AFM, and XPS studies," *Journal of Molecular Liquids*, vol. 216, pp. 164–173, 2016.

[43] P. Preethi Kumari, P. Shetty, and S. A. Rao, "Electrochemical measurements for the corrosion inhibition of mild steel in 1 M hydrochloric acid by using an aromatic hydrazide derivative," *Arabian Journal of Chemistry*, vol. 10, no. 5, pp. 653–663, 2017.

[44] M. Chellouli, D. Chebabe, A. Dermaj et al., "Corrosion inhibition of iron in acidic solution by a green formulation derived from Nigella sativa L.," *Electrochimica Acta*, vol. 204, pp. 50–59, 2016.

[45] J. Bhawsar, P. K. Jain, and P. Jain, "Experimental and computational studies of *Nicotiana tabacum* leaves extract as green corrosion inhibitor for mild steel in acidic medium," *Alexandria Engineering Journal*, vol. 54, no. 3, pp. 769–775, 2015.

[46] S. A. Umoren and M. M. Solomon, "Recent developments on the use of polymers as corrosion inhibitors - a review," *The Open Materials Science Journal*, vol. 8, no. 1, pp. 39–54, 2014.

[47] C. B. Verma, P. Singh, I. Bahadur, E. E. Ebenso, and M. A. Quraishi, "Electrochemical, thermodynamic, surface and theoretical investigation of 2-aminobenzene-1,3-dicarbonitriles as green corrosion inhibitor for aluminum in 0.5 M NaOH," *Journal of Molecular Liquids*, vol. 209, article no. 4922, pp. 767–778, 2015.

[48] D. K. Yadav, B. Maiti, and M. A. Quraishi, "Electrochemical and quantum chemical studies of 3,4-dihydropyrimidin-2(1H)-ones as corrosion inhibitors for mild steel in hydrochloric acid solution," *Corrosion Science*, vol. 52, no. 11, pp. 3586–3598, 2010.

[49] M. Yadav, L. Gope, and T. K. Sarkar, "Synthesized amino acid compounds as eco-friendly corrosion inhibitors for mild steel

in hydrochloric acid solution: Electrochemical and quantum studies," *Research on Chemical Intermediates*, vol. 42, no. 3, pp. 2641–2660, 2016.

[50] P. M. Dasami, K. Parameswari, and S. Chitra, "Corrosion inhibition of mild steel in 1MH2SO4 by thiadiazole Schiff bases," *Measurement*, vol. 69, pp. 195–201, 2015.

[51] X. Li, S. Deng, H. Fu, and T. Li, "Adsorption and inhibition effect of 6-benzylaminopurine on cold rolled steel in 1.0 M HCl," *Electrochimica Acta*, vol. 54, no. 16, pp. 4089–4098, 2009.

[52] A. Popova, M. Christov, S. Raicheva, and E. Sokolova, "Adsorption and inhibitive properties of benzimidazole derivatives in acid mild steel corrosion," *Corrosion Science*, vol. 46, no. 6, pp. 1333–1350, 2004.